ELSEVIER

Biochimica et Biophysica Acta 1324 (1997) 1–17

BIOCHIMICA ET BIOPHYSICA ACTA
BBA

Phase behavior of fluorocarbon di-*O*-alkyl-glycerophosphocholines and glycerophosphoethanolamines and long-term shelf stability of fluorinated liposomes

Véronique Ravily [a], Catherine Santaella [a], Pierre Vierling [a,*], Annette Gulik [b]

[a] *Laboratoire de Chimie Moléculaire, URA CNRS 426 and Laboratoire de Chimie Bioorganique, EP CNRS 104, Faculté des Sciences, Université de Nice-Sophia Antipolis, B.P. 71, 06108 Nice Cédex 2, France*
[b] *Centre de Génétique Moléculaire, CNRS, 91190 Gif sur Yvette, France*

Received 21 May 1996; revised 18 September 1996; accepted 24 September 1996

Abstract

This paper is devoted to the morphological characterization, by freeze-fracture electron microscopy, and to the thermotropic phase behavior, by differential scanning calorimetry and X-ray diffraction of the aqueous dispersions of various fluorocarbon/fluorocarbon or mixed fluorocarbon/hydrocarbon 1,2- or 1,3-di-*O*-alkyl-glycerophosphocholines (PC) and 1,2-di-*O*-alkyl-glycerophosphoethanolamines (PE). The fluorinated PCs form classical lamellar phases and liposomes while an interdigitated lamellar phase has been evidenced for a hydrocarbon 1,3-analog. The fluorinated PEs display a lamellar to hexagonal phase transition which occurs almost simultaneously with the gel-to-fluid lamellar phase transition. The impact of each of the structural features [ether vs ester chemical junction connecting the hydrophobic chains on glycerol, their position (1,2- vs 1,3 isomers), number and length of the perfluoroalkylated chains, length of the fluorinated tail and hydrocarbon spacer, PC vs PE polar head] of the fluorinated phospholipids on the phase transition thermodynamic parameters (Tc, ΔH, ΔS) is discussed. Most of the liposomes formed from the fluorinated ether-PCs display a remarkable long-term shelf stability: they can be thermally sterilized and stored at room temperature for several months without any significant modification of their size and size distribution.

Keywords: Perfluoroalkylated phospholipid; Fluorinated liposome; Vesicle; Membrane; Polymorphism; Shelf-stability

1. Introduction

Liposomes (vesicles made from phospholipids) provide challenging in vivo delivery systems for enhancing the efficacy of various biologically active materials [1,2], reducing the toxicity of various anti-tumor agents, facilitating intracellular drug delivery, increasing the tumoricidal activity of macrophages and enhancing the immune response and thus serve as artificial vaccines [1]. Much effort has been focused in more recent years on liposomes with increased residence in the bloodstream (e.g., 'stealth' liposomes) [2,3]. Progress in this field has allowed specific drug targeting to cells and organs [1–3].

The elaboration of liposomal systems with new or significantly improved properties implies the devel-

* Corresponding author. Fax: +33 4 92 076151. E-mail: vierling@unice.fr

PII S0005-2736(96)00203-9

opment of components that are substantially different from those currently utilized. Highly fluorinated phospholipids (Fig. 1) are such components: they offer some of the specific features that make up the uniqueness of fluorinated material, e.g., their hydrophobic *and* lipophobic character [4]. The fluorinated DFnCmPC phosphatidylcholines (Fig. 1, [5]) were shown to form liposomes [6–8], their fluorinated tails creating inside the liposomal membrane a highly hydrophobic and lipophobic fluorocarbon layer. This layer modifies substantially the phase behavior characteristics [7] and dynamics [9], reduces membrane permeability [10], increases the stability of the liposomes in biological media (in terms of release

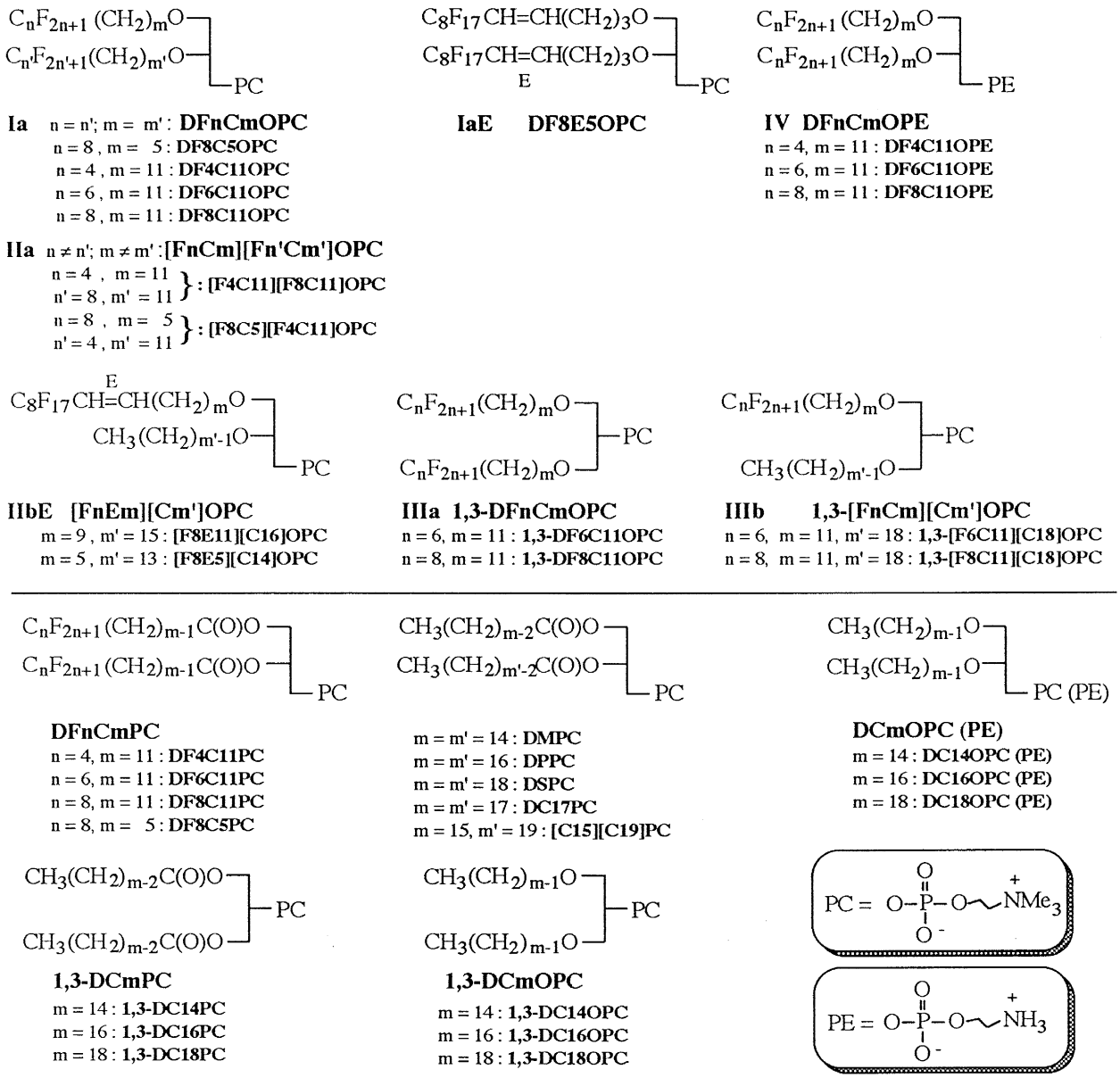

Fig. 1. Chemical structure and code name of the various fluorocarbon 1,2- and 1,3-di-*O*-alkyl-(ether-connected) glycerophosphocholines and glycerophosphoethanolamines together with those of the various fluorocarbon di-*O*-acyl-(ester-connected)-glycerophosphocholines and hydrocarbon analogs used as references throughout this study.

of encapsulated material) [10] and, importantly, prolongs their in vivo blood circulation times [11].

In order to further act on and modulate the hydrophobic-lipophobic/lipophilic/hydrophilic balance, and consequently, the physico-chemical and biological properties of fluorinated membranes and liposomes (thermotropism, lipid mobility, order and packing, permeability, stability in biological fluids, interactions with bio-compounds, in vivo fate), we have recently extended the range of fluorinated phospholipids by performing the synthesis of various perfluoroalkylated 1,2- and 1,3-di-*O*-alkyl (ether-connected) glycerophospholipids (Fig. 1) [12]. Their molecular structures follow a modular design, which allows incremental structural variations aimed at the establishment of structure/properties relationships. This design involves two hydrophobic chains, one (**IIb** and **IIIb**) or both (**Ia**, **IaE**, **IIa**, **IIIa** and **IV**) of which end in a highly fluorinated tail, in combination with saturated (**Ia**, **IIa**, **IIbE** and **III**–**IV**) and/or unsaturated (**IaE** and **IIbE**) aliphatic chains connected through glycerol to phosphocholine (PC) (**I**–**III**) or phosphoethanolamine (PE) (**IV**) polar head groups.

This paper is devoted to the polymorphic phase behavior of these perfluoroalkylated di-*O*-alkylglycerophospholipids in water. Such a study is a prerequisite when their use as liposomal components is intended. The morphological characterization of the supramolecular structures they form and their thermotropic phase behavior was performed by freeze-fracture electron microscopy (FFEM) and by differential scanning calorimetry (DSC) or X-ray diffraction, respectively. The impact of each of the structural features which composes the molecular structure of the fluorinated phospholipids on the phase transition thermodynamic parameters is furthermore discussed. In all cases, the experimental data obtained are compared with those reported for their fluorinated ester (DFnCmPC), hydrocarbon ester and ether analogs (Fig. 1). In addition, the size and size distribution of the liposomes they form and their long-term shelf stability with respect to particle size evolution after a standard heat-sterilization process and storage at room temperature (analyzed by light scattering spectroscopy, LSS) are also described. These are key issues when the use of liposomes as drug carrier and delivery devices is contemplated.

2. Materials and methods

The synthesis and characterization (elemental analysis, ^{1}H, ^{13}C, ^{31}P, ^{19}F NMR) of the fluorinated ether-connected glycerophospholipids (Fig. 1) used in this study are described in Ref. [12]. Their purity ($> 99\%$) was periodically checked by TLC. Rac-dipalmitoylphosphatidylcholine (DPPC, 99%), egg phosphatidylcholines (EPC) and cholesterol (CH) were supplied by Fluka, Lipoid and Sigma, respectively, and used without further purification. Dispersions of the lipids were prepared with a Branson B-30 sonifier. Alternatively, extrusion through a polycarbonate membrane (Liposofast Milsch Equipment; size filter 100 nm) was also used to prepare liposomes. Particle sizes and size distributions were determined by LSS on a Coulter N4SD Sub-Micron Particle Analyser.

2.1. Preparation of the dispersions and liposomes

For the observation by optical microscopy with polarized light (Olympus BH2), the samples were prepared by dispersion (vortex) of the lipid in excess water at room temperature, then placed onto the microscope between two glasses which were heated progressively.

For the FFEM studies, unilamellar vesicles (concentration of phospholipid 30 mM) were prepared, by sonication or by extrusion, in a phosphate-buffered saline (PBS, BioMérieux) as described in Ref. [10] and were aged for 10–12 h at a temperature 5–10°C above the phase transition temperature, Tc, detected by DSC, of the phospholipid under investigation.

For the stability studies, 5-ml samples (10 mM) were prepared by sonication or extrusion, then sterilized by autoclaving the dispersions for 15 min at 121°C under a pressure of 15 lb/sq.in in an oscillating autoclave (Subtil, Crépieux) and stored at 25 (± 1)°C. Average vesicle size measurements were performed by LSS after preparation, after heat-sterilization, then periodically during storage.

2.2. Freeze-fracture electron microscopy (FFEM)

The dispersions were prepared as described above and stored at room temperature for three days before analysis. To prevent freeze damage, the samples were

diluted with an equivalent volume of an aqueous solution of glycerol (50% w/w) and incubated at room temperature for 4 h before cryofixation. A small drop of each suspension (about 0.5 μl) was deposited on a thin copper holder and then quenched in liquid propane. The frozen sample was fractured at -125°C in vacuo (about 10^{-7} Torr) with a liquid nitrogen-cooled knife in a Balzers 301 freeze-etching unit. The fractured sample was replicated with platinum-carbon (1–1.5 nm of metal deposit) backed with about 20 nm of carbon and the replica was cleaned with organic solvents, washed with distilled water and observed with a Philips 301 electron microscope. For each sample, two or three independent freezings, fractures and replicas were realized.

2.3. Differential scanning calorimetry (DSC)

For DSC measurements in the $+4$ to 95°C and -25 to $+4$°C temperature range, the samples were prepared by weighing the powdered phospholipid (2–3 mg) into the DSC inox pan and adding a weighed amount of deionized water or of an ethyleneglycol/water (70/30 w/w) solution (4–6 mg), respectively. DSC measurements were carried out with Perkin Elmer DSC-2 and DSC-7 differential scanning calorimeters. Each sample was heated and cooled repeatedly at a rate of 2–5°C/min and 10°C/min respectively. Transition enthalpies and temperatures were determined after several heating/cooling cycles. The reported values of the

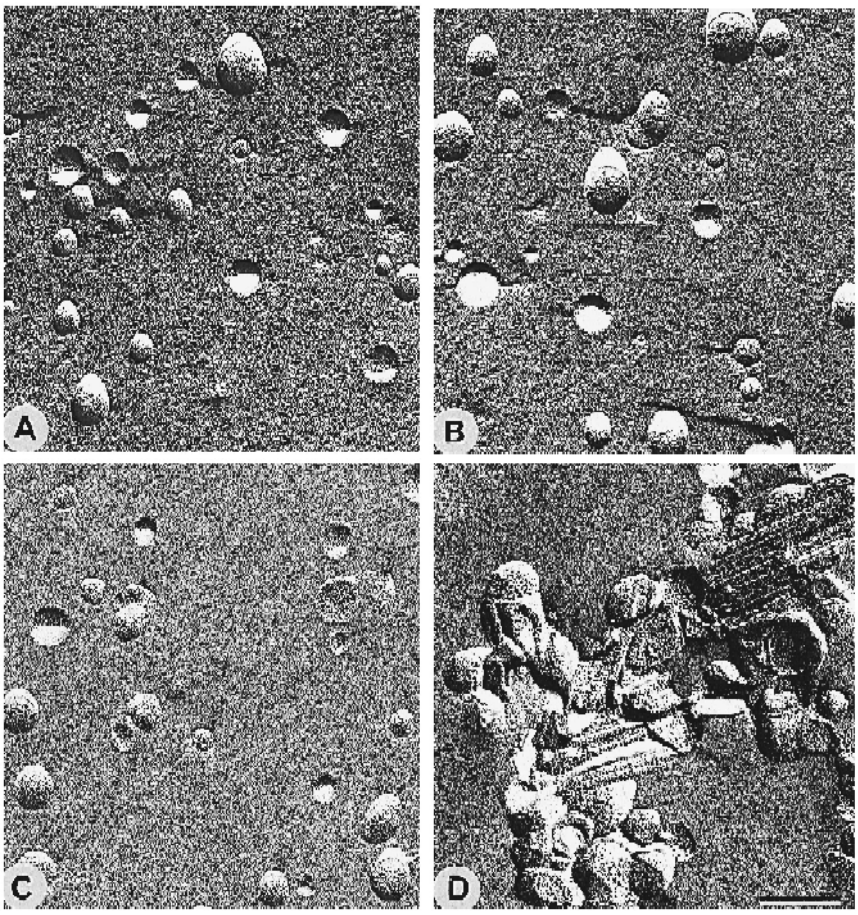

Fig. 2. A–D: Freeze fracture electron micrographs of 4% w/w aqueous liposomal dispersions of (A) [F8E11][C16]OPC, (B) 1,3-[F6C11][C18]OPC, (C) [F4C11][F8C11]OPC and (D) DF6C11OPC showing the simultaneous presence of ribbon-like elements and vesicles. Scale bar is 200 nm.

Tc represent the temperature at maximum excess heat capacity.

2.4. X-ray scattering

The samples were prepared by mixing the lipid and excess water. In order to obtain the best hydration of the lipids, it was performed by incubating the resulting suspensions at 70°C for DF4C11OPE and 90°C for DF6C11OPE. The samples were then mounted in vacuum-tight cells with mica windows. The Debye-Scherrer spectra were recorded using a Guinier-type focussing camera with a bent quartz monochromator. The spectra were recorded at selected temperatures or continuously as a function of temperature.

3. Results and discussion

3.1. FFEM and LSS studies of the fluorinated phospholipid dispersions

As shown by FFEM (Fig. 2A–C), the aqueous dispersions of DF8C5OPC (not shown), [F4C11][F8C11]OPC, [F8E11][C16]OPC and 1,3-[F6C11][C18]OPC performed by extrusion or sonication consist mainly in unilamellar vesicles. Each of these compounds being representative of a distinctive family of the fluorinated ether-connected PCs, it appears that formation of liposomes is neither affected by the number (one or two) of fluorinated chains nor by the connection in the 1,2- or 1,3-position on glycerol of the two hydrophobic chains.

The same dispersions were also analyzed by LSS. The vesicles of DF8C5OPC obtained by sonication, had an average particle size of 50 nm and were polydisperse. By contrast, the liposomes formed by each of the other fluorinated lipids prepared by extrusion through a 100-nm polycarbonate membrane, had a homogeneous particle size distribution centered around 100 nm, in agreement with FFEM (see Fig. 2A–C).

By contrast to the above mentioned dispersions, those of DF6C11OPC, DF8C11OPC, 1,3-DF6C11OPC or 1,3-DF8C11OPC were shown to consist in vesicles which slowly convert into a ribbon-like phase at room temperature. The coexistence of vesicles with this phase is illustrated in Fig. 2D for DF6C11OPC. Such a ribbon phase has already been observed by FFEM and confirmed by X-ray diffraction for the DF6C11PC and DF8C11PC ester analogs [7]. It should be mentioned that this phase is only observed for phosphocholines having a fluorinated tail on both hydrophobic chains and each chain having at least 17 carbon atoms. Indeed, a ribbon phase is neither found for [F4C11][F8C11]OPC, [F8E11][C16]OPC nor for 1,3-[F6C11][C18]OPC which has two chains equal to or longer than 17 carbon atoms.

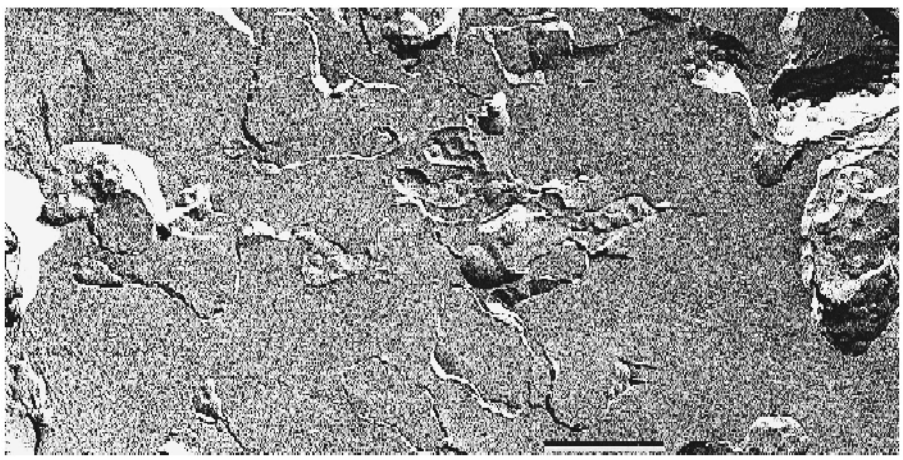

Fig. 3. Freeze-fracture image of a 4% w/v viscoelastic gel (viscous solution) obtained by cooling to room temperature an aqueous liposomal dispersion of 1,3-DC18OPC. Scale bar is 500 nm.

The fluorinated 1,3-di-*O*-alkylglycero-2-phosphocholines which form vesicles and/or a ribbon phase display a behavior which differs from that observed for their hydrocarbon analog 1,3-DC18OPC. After sonication at a temperature above its phase transition temperature, 1,3-DC18OPC forms a translucent dispersion consisting in liposomes which leads to a viscoelastic gel (viscous solution) after cooling to room temperature (a replica of this dispersion is shown in Fig. 3). The formation of a gel and its appearance on the micrographs seems to be the result of some fusion of the liposomes. This fusion may be related to the low stability of the rather small-sized vesicles and/or to the transition from a conventional lamellar ($L\beta$ or $L\beta'$) to an interdigitated lamellar phase ($L\beta i$). Upon cooling, whereas a part of the chains remains non-interdigitated, another part interdigitates as evidenced by the FFEM images which show both usual fractures along the mid-plane of the membrane (convex and concave liposomes) and cross-fractures, respectively. The formation of a gel interdigitated lamellar $L\beta i$ phase in excess of water for 1,3-DC18OPC has been further confirmed by X-ray diffraction [13] and is in line with the phase behavior of other ether-linked glycerophosphocholines, such as DC16OPC [14], or of the 1,3-isomer of the ester-linked DPPC [15].

The absence of an interdigitated lamellar $L\beta i$ phase for the fluorinated ether-PCs thus constitutes the main difference with their hydrocarbon 1,3-DC18OPC or DC16OPC analogs. Indeed, none of our FFEM micrographs recorded for the fluorinated ether-PCs has shown the presence of cross-fractures which are typical of an interdigitated lamellar phase. The formation of a classical gel lamellar phase for several of the fluorinated ether-PCs investigated here has been further confirmed by a X-ray diffraction study [16].

3.2. Thermotropic phase behavior of the fluorocarbon di-O-alkyglycerophosphocholine (PC) derivatives

The thermotropic phase behavior of samples consisting of hydrated powders of the fluorinated PCs was studied by DSC. Thus, when samples of the

Table 1
Thermodynamic parameters of the phase transitions for the perfluoroalkylated 1,2-di-*O*-alkylglycero-3-phosphocholines and their hydrocarbon DCmOPC analogs

Compound	Pre-transition			Main phase transition $L_{\beta'}$ (or $P_{\beta'}$) tp L_{α}		
	T (±1°C) ($\Delta T_{1/2}$) [e]	ΔH(±5%) (kJ/mol)	ΔS (J/mol.K)	Tc (±1°C) ($\Delta T_{1/2}$) [e]	ΔH (±5%) (kJ/mol)	ΔS (J/mol.K)
DF8C5OPC [a]	–	–	–	60 (2)	6.7	20.3
DF8E5OPC [a]	[b]	–	–	[b]	–	–
DF4C11OPC [a]	–	–	17 (3)	11.1	38.3	
DF6C11OPC [a]	43 (4)	9.1	28.8	50 (4)	12.6	39.0
DF8C11OPC [a,c]	–	–	–	88 (2)	28	78
[F8C5][F4C11]OPC [a]	–	–	–	10 (large)	not measurable	
[F4C11][F8C11]OPC [a,c]	33 (2)	0.6	1.9	36 (2)	3.3	10.7
				40 (2)	5.5	17.6
[F8E5][C14]OPC [a]	–	–	–	< −25	–	–
[F8E11][C16]OPC [a]	–	–	–	5 (3)	7.7	27.7
[F8C11][C16]OPC [a]	32 (4)	1.1	3.6	44 (4)	8.2	25.9
DC14OPC [d]	–	–	–	27	30.9	103.7
DC16OPC [d]	–	–	–	43–45	38.4	123.2
DC18OPC [d]	–	–	–	55	41.8	128.2

[a] DSC measurements were performed in water (60% w/w); for DF4C11OPC, the content of water was 70% w/w.
[b] No transition detected between −25 and +95°C.
[c] Each transition is split in two after several heating/cooling cycles.
[d] From Ref. [17] and refs. therein.
[e] $\Delta T_{1/2}$ is the transition width at half-maximal excess specific heat capacity.

various compounds shown in Fig. 1 are heated from −25°C (or from 4°C) up, in most cases a main phase transition and, in some cases, a pretransition of lower energy are observed reproducibly, even after the sample was taken repeatedly through several heating-cooling cycles. Tables 1 and 2 collect the thermodynamic parameters – phase transition temperature, Tp (pretransition) and Tc (gel to fluid main phase transition, vide infra), and their associated enthalpy, ΔH, and entropy, ΔS, for the fluorinated di-*O*-alkyglycerophosphocholines together with those corresponding to their most direct hydrocarbon ether (DCmOPC) [17], fluorinated (DFnCmPC) [7] and hydrocarbon ester phosphatidylcholine (DMPC, DPPC and DSPC [18]) analogs (see Fig. 1) which are taken as references for the discussion in Section 3.3.

As supported by X-ray diffraction [16], FFEM (vide supra) and optical microscopy with polarized light, and by analogy with the thermotropic phase behavior of their DFnCmPC analogs [7], the various fluorinated ether-connected PCs form lamellar phases, when dispersed in an aqueous phase. Thus, optical microscopy performed on the hydrated powders, when heating the samples through the highest phase transition temperatures listed in Tables 1 and 2, showed the appearance of the characteristic optical pattern of Maltese crosses, which indicates that the fluorinated PCs are typically organized in a liquid-crystalline or fluid ($L\alpha$) lamellar phase above these temperatures and that a phase transition from a lamellar $L\beta(\beta')$ or rippled $P\beta(\beta')$ gel phase has most likely occurred. When two phase transitions are detected by DSC, the less energetic pretransition and the higher energetic transition can thus be assigned to a transition from a lamellar $L\beta(\beta')$ to a rippled gel $P\beta(\beta')$ phase and from a rippled gel to a lamellar $L\alpha$ transition, respectively. The unique phase transition observed for several PCs is a transition from a $L\beta(\beta')$ phase to a $L\alpha$ phase (or a $P\beta(\beta')$ to $L\alpha$ phase transition, if the L to P pretransition is energetically too low to be detected). This analysis is in full agreement with our X-ray diffraction study [16] which showed, at 23°C, a gel lamellar $L\beta'$ phase for [F8C11][C16]OPC, 1,3-DF6C11OPC, 1,3-[F8C11][C16]OPC, or 1,3-[F8C11][C18]OPC, and a fluid lamellar phase for [F8E11][C16]OPC. In the case of the phospholipids which also form a ribbon-like phase, one of the transitions detected by DSC could arise from a ribbon-like to a lamellar phase transition. However, this transition is only slowly reversible (several days [7]). Furthermore, the pre- and main phase transitions are always measured by DSC, even after several heating/cooling cycles. This most likely indicates that none of these transitions can be assigned to a ribbon-like/lamellar phase transition.

Table 2
Thermodynamic parameters of the phase transitions for the perfluoroalkylated 1,3-di-*O*-alkylglycero-2-phosphocholines and their hydrocarbon analogs 1,3-DCmOPC

Compound	Pre-transition			Main phase transition $L_{\beta'}$ (or $P_{\beta'}$) to L_{α}		
	T (±1°C) ($\Delta T_{1/2}$)	ΔH (kJ/mol) (±5%)	ΔS (J/mol.k)	T (±1°C) ($\Delta T_{1/2}$)	ΔH (kJ/mol) (±5%)	ΔS (J/mol.k)
1,3-DF6C11OPC [a,b]	46 (1)	5.5	17.2	52 (2)	11.3	34.8
1,3-DF8C11OPC [a]	–	–	–	87 (2)	18.1	50.1
1,3-[F6C11][C18]OPC [a]	–	–	–	39 (2)	28.9	92.8
1,3-[F8C11][C18]OPC [a]	44 (2)	3.5	11.0	46 (3)	17.7	55.4
1,3-DC14OPC [c]	–	–	–	29	25.9	85.9
1,3-DC16OPC [c]	–	–	–	33	25.1	82.0
1,3-DC18OPC [a]	–	–	–	59 (1)	43.0	129.7
				59 [c]	46.8 [c]	

[a] DSC measurements were performed in water (60% w/w).
[b] Each transition is split in two after several heating/cooling cycles.
[c] From Ref. [17].
[d] $\Delta T_{1/2}$ is the transition width at half-maximal excess specific heat capacity.

It should be mentioned that the main phase transitions of the fluorinated phospholipids are much broader than those measured for DMPC, DPPC or DSPC (see transition width at half-maximal excess specific heat capacity, $\Delta T1/2$, values listed in Tables 1 and 2). Furthermore, the longer the Fn tail the larger the phase transition, hence the lower its cooperativity. This has also been shown for the DFnCm-PCs for which it has been established that the phase transition is first induced by the melting of the Fn tail and that each portion of the Fn tail and the hydrocarbon Cm spacer experiences intrinsic changes of molecular motion with temperature [7]. That the melting of the perfluoroalkyl chains occurs over a large temperature range (up to 20°C for a F8Cm chain from the onset to completion) is thus in marked contrast with the hydrocarbon phosphatidylcholine's behavior for which chain melting, due to high cooperativity, occurs within a very short temperature range (1°C) at their phase transition temperature [19].

By contrast, the heating curves of samples of DF8E5OPC or [F8E5][C14]OPC showed no observable phase transition in the −25 to 95°C temperature range. Thus, the DSC experiments most likely indicate that the gel to fluid phase transition occurs, for these compounds, at a temperature either lower than −25°C or in the −25 to 95°C range with an enthalpy too weak to allow its detection. Both compounds possess an ethylenic bond in each or in one of their hydrophobic chains and are mixtures of *cis/trans* isomers (*cis/trans* ratio of 20/80 and 10/90, respectively) [12]. This is expected to broaden the phase transition and to lower the thermodynamic parameters, as compared to those of their saturated analogs [18,20] (see also our discussion concerning this aspect in Section 3.4.4.). The fact that no phase transition was observed for DF8E5OPC in the −25 to 95°C temperature range could thus result from a subsequent broadening of the phase transition of DF8C5OPC (which is already very large) and from a decrease in ΔH which make the detection of the phase transition very difficult or even impossible. This latter situation is further supported by the thermotropic behavior of DF6E11PC (*cis/trans* ratio of 20/80) which displays a much broader and energetically much lower phase transition than its saturated DF6C11PC analog [6]. When considering the fact that a decrease in chain length is generally accompanied by a decrease in Tc and in ΔH [18,19], [F8E5][C14]OPC, whose hydrophobic chains are shorter than those of [F8E11][C16]OPC by six and two methylenic carbon atoms, is therefore expected to exhibit lower thermodynamic phase transition parameters than those of [F8E11][C16]OPC (Tc = 5°C,

Table 3
Thermodynamic parameters of the phase transitions for the fluorinated 1,2-di-*O*-alkyglycerophosphoethanolamines DFnCmOPE and their hydrocarbon DCmOPE analogs

Compound	$L_{\beta'}$ to L_α or H_{II} Transition			L_α to H_{II} Transition		
	Tc (±1°C) ($\Delta T_{1/2}$) [g]	ΔH (±5%) (kJ/mol)	ΔS (J/mol.K)	T (±1°C)	ΔH (±5%) (kJ/mol)	ΔS (J/mol.K)
DF4C11OPC [a]	32 (3) 31 (2) *	20.2	66.2	[d]	–	–
DF6C11OPE [a]	63 (5)	20.3	60.4	e	–	–
DF8C11OPE [a,b]	94 (5)	15.7	43.0			
DC14OPE [f]	56	24	73	96	3	8.2
DC16OPE [f]	69	33.1	97	86	6.1	16.9
DC18OPE [f]	77	39.1	112	81	6.9	19.5

[a] DSC measurements were performed in Hepes/NaCl 0.15 M (pH 7.3) buffer (60% w/w); * in water (60% w/w).
[b] A pre-transition is detected at 85°C ($\Delta H = 0.9$ kJ/mol).
[c] The exact nature of this transition is not clearly established.
[d] No transition detected above 32°C.
[e] No transition detected above 63°C.
[f] From Ref. [21].
[g] $\Delta T_{1/2}$ is the transition width at half-maximal excess specific heat capacity.

$\Delta H = 7.7$ kJ/mol). This indicates that the main phase transition of [F8E5][C14]OPC most likely occurs at a temperature below -25°C.

3.3. Thermotropic phase behavior of the fluorocarbon di-O-alkyglycerophosphoethanolamine (PE) derivatives

The thermotropic phase behavior of samples consisting of hydrated powders of the fluorinated ether-PEs was investigated by DSC and X-ray scattering. Table 3 collects the thermodynamic parameters determined by DSC – Tc (gel to fluid main phase transition and/or lamellar to hexagonal phase transition, vide infra), and their associated ΔH and ΔS – on these dispersions together with those reported for their most direct hydrocarbon ether DCmOPE analogs (Fig. 1) [21] which are taken as references for the discussion in Section 3.4.

Our X-ray diffraction study performed on hydrated DF4C11OPE or DF6C11OPE as a function of temperature showed that above 28°C and at 70°C, respectively, these compounds, in excess water, form a hexagonal phase. This is supported by the observation of a set of five reflections in the spacing ratio of $1/\sqrt{3}/\sqrt{7}/\sqrt{12}/\sqrt{13}$ for DF4C11OPE and of $1/\sqrt{3}/\sqrt{4}/\sqrt{7}/\sqrt{13}$ for DF6C11OPE corresponding to a cell dimension of 75.0 Å and 73.2 Å, respectively. Below the temperature domain of the hexagonal phase, the low-angle scattering spectra were more or less complex, depending on the history of the sample, and exhibited either sharp reflections or, when recorded after a long storage period at room temperature, both sharp and broad reflections. Among the sharp reflections, some indexed as orders of a lamellar repeat period, which we take to indicate that the fluorinated PEs form a bilayer structure which coexists with (an)other phase(s). The rather complex wide-angle scattering regions for DF4C11OPE and DF6C11OPE, with a mixture of sharp and broad reflections, could further indicate the presence of a gel phase bilayer [22]. Indeed, a broad band extending from 5.4 to 4.5 Å^{-1} with a sharp inner edge at 5.4 Å^{-1} and a superimposed reflection at 5.0 Å^{-1}, and two broad bands extending from 5.4 to 5.0 Å^{-1} and 4.6 to 4.3 Å^{-1} together with a sharp inner reflection at 5.4 Å^{-1} were measured for DF4C11OPE and DF6C11OPE, respectively. The dependence of the X-ray diffraction patterns on the sample history is most probably related to the amount of water that enters/remains within the different phases. This could also account for the discrepancy with the phase transition temperature as detected by DSC.

Furthermore, the presence of the characteristic optical pattern of Maltese crosses by optical microscopy with polarized light of their hydrated powders incubated at a temperature close to their phase transition temperature indicated in Table 3, suggests that the fluorinated PEs are also organized in a fluid lamellar phase.

All these results most likely indicate that the unique and broad phase transition (ΔT1/2 of 4–5°C) observed by DSC for the fluorinated PEs consists in a superposition of transitions, among which one can recognize the lamellar gel to fluid phase transition followed, almost simultaneously, by a transition to a hexagonal phase. Their thermotropic phase behavior thus resembles, to some extent, that of their hydrocarbon analogs apart from the fact that both the lamellar gel to fluid and lamellar to hexagonal phase transitions occur for the fluorinated PEs at very close temperatures.

In the hydrocarbon phosphatidylcholine series, replacing the phosphocholine polar head by a phosphoethanolamine one results in a subsequent increase of the gel to fluid lamellar phase transition temperature and in the appearance of a transition from a lamellar to an inverted hexagonal H_{II} phase [18,19,22,23]. These two facts are also found when going from the fluorinated PC to the fluorinated PE series. Concerning more particularly Tc and as illustrated in Fig. 4c, the DFnC11OPCs do indeed display lower Tcs than their respective DFnC11OPE analogs. However, one can observe that the magnitude in Tc increase when going from the PC to the PE series is less important for the fluorocarbon than for the hydrocarbon derivatives. Formation of a lamellar phase or of a hexagonal H_{II} phase is favored when the size of the polar head is similar or smaller to that of the hydrophobic part, respectively. The PE head cross-section being smaller than that of a PC head and of the two hydrocarbon chains in the glycerophospholipids, and this size disproportion becoming even larger when hydrocarbon chains are replaced by fluorocarbon ones (cross-sectional area of about 30 Å^2 for a fully extended alkyl chain of CF_2 groups compared to the

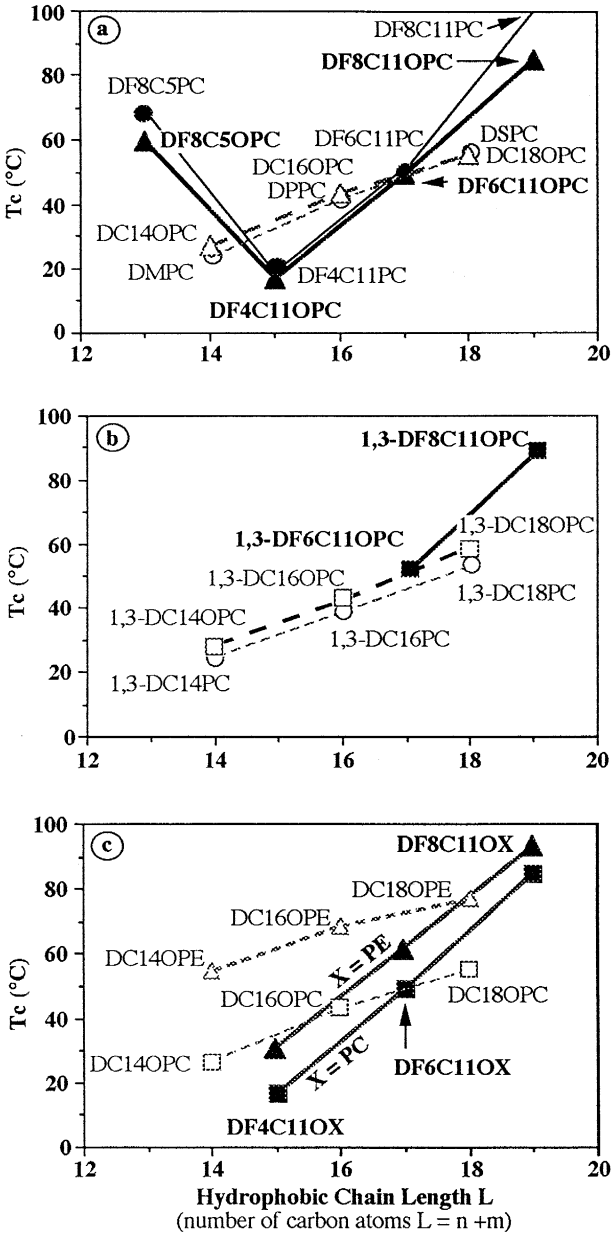

Fig. 4. a–c: Evolution of the phase transition temperature, Tc, with the length, L, of the fluorocarbon (filled symbols) or hydrocarbon (open symbols) hydrophobic chains: (a) in the 1,2-di-*O*-alkyl- (▲, △) and 1,2-di-*O*-acyl-glycero-3-phosphocholine (●, ○) series, (b) in the 1,3-di-*O*-alkyl- (■, □) and 1,3-di-*O*-acyl- (○) glycero-2-phosphocholine series, (c) in the 1,2-di-*O*-alkylglycero-3-phosphoethanolamine (▲, △) and -choline (■, □) series. Data of the fluorocarbon (DFnCmPC), hydrocarbon (DMPC, DPPC and DSPC) 1,2-di-*O*-acyl-glycero-3-phosphocholines and hydrocarbon 1,3-di-*O*-acyl-glycero-2-phosphocholines are taken from Refs. [7] and [18], respectively. * L represents the number of carbon atoms of the fluorinated tail (n) and hydrocarbon spacer (m) or of the hydrocarbon (m) alkyl or acyl chain.

20 Å^2 for a chain of CH_2 [25,26]), one expects therefore that the formation of an inverted hexagonal phase is much more favored for PEs having fluorocarbon chains. This is what we observe. Indeed, the lamellar to hexagonal phase transition occurs at much lower temperatures when replacing, in the fluorinated series, the PC head for a PE one.

3.4. Structure / phase transition thermodynamic parameter relationships

It is well known that the Lβ (Lβ' or Pβ(β') to Lα phase transition of the lipid bilayer detected by DSC is an energetic event reflecting a cooperative transition of the bilayers from an ordered gel state to a disordered fluid state at Tc. The relative energetic contents and hence the relative packing modes of the lipid chains between two lipid bilayer systems can thus be compared on the basis of their thermodynamic parameters associated with the main phase transitions. The packing modes of the chains can be conveniently described in terms of the conformational statistics (trans/gauche ratio), lateral chain-chain and hydrophobic interactions. Consequently the observed changes in Tc, ΔH and ΔS values associated with the main phase transition may be attributed primarily to differences in the conformational statistics of the chains, lateral chain-chain and hydrophobic interactions of the respective PCs or PEs in the gel state.

One of the main objectives of this study was to determine the impact on the phase transition thermodynamic parameters (Tc, ΔH, ΔS) of several structural elements – nature of the chemical junction (ester vs ether) and polar head (PC vs PE, which has already been discussed above in Section 3.3.), position of the hydrophobic chains on glycerol (1,2- vs 1,3 isomers), number and length of the perfluoroalkylated chains, length of the fluorinated tail and hydrocarbon spacer. The following discussion is organized according to these criteria.

3.4.1. Impact of the ester / ether junction

Fig. 4a which represents the variations of Tc in the ester and ether series shows that no major difference exists for the DF4C11PC/DF4C11OPC pair. However, a more important difference can be noted for compounds whose hydrophobic chains are ended by a

F6 or F8 tail. Thus, it was found that the DF6C11OPC, DF8C5OPC and DF8C11OPC ethers display lower Tc values than their corresponding ester analogs (respectively by 6, 9°C and even more for the DF8C11OPC/DF8C11PC couple). This tendency is thus opposite to that which is observed in the hydrocarbon ester and ether series: the latter display slightly higher Tc values (~0 to 5°C) than their ester analogs due to a tighter chain–chain packing owing to the absence of the carbonyl groups [24]. The closer chain–chain packing, when going from the ester to the ether series, more than outweighs the loss of inter- and intramolecular hydrogen bonding interactions which involves the carbonyl groups and water molecules. For the fluorocarbon series, the greater steric hindrance of the F6 and F8 tails, as

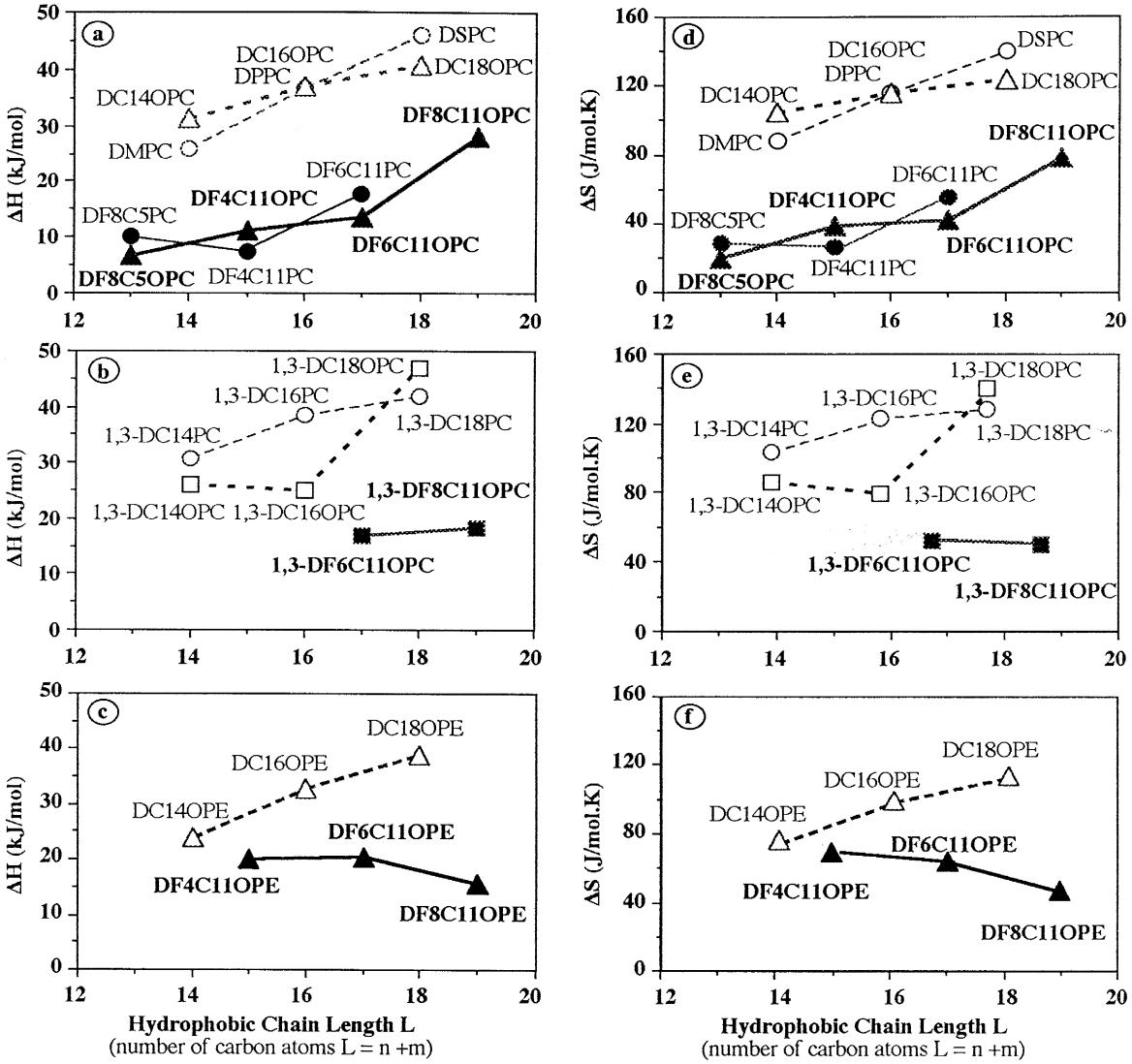

Fig. 5. a–f: Evolution of the phase transition enthalpy, ΔH (a–c), and entropy, ΔS (d–f), with the length, L, of the fluorocarbon (filled symbols) or hydrocarbon (open symbols) hydrophobic chains: (a,d) in the 1,2-di-*O*-alkyl- (▲, △) and 1,2-di-*O*-acyl-glycero-3-phosphocholine (●, ○) series; (b,e) in the 1,3-di-*O*-alkyl- (■, □) and 1,3-di-*O*-acyl-glycero-2-phosphocholine (○) series; (c,f) in the 1,2-di-*O*-alkylglycero-3-phosphoethanolamine (▲, △) series. Data of the fluorocarbon (DFnCmPC) and hydrocarbon (DMPC, DPPC and DSPC) 1,2-di-*O*-acyl-glycero-3-phosphocholines and 1,3-di-*O*-acyl-glycero-2-phosphocholines are taken from Refs. [7] and [18], respectively. * L represents the number of carbon atoms of the fluorinated tail (n) and hydrocarbon spacer (m) or of the hydrocarbon (m) alkyl or acyl chain.

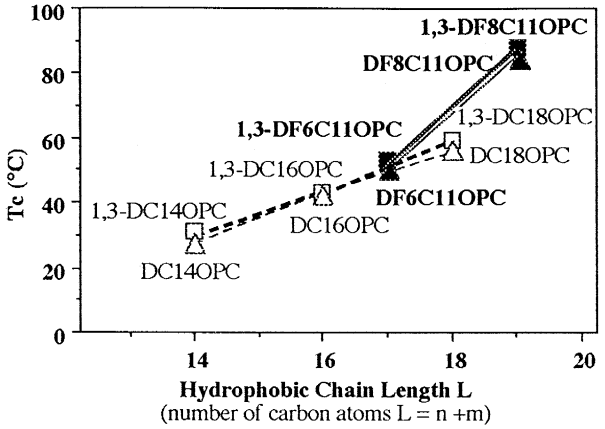

Fig. 6. Evolution of the phase transition temperature, Tc, with the length, L, of the fluorocarbon (filled symbols) or hydrocarbon (open symbols) hydrophobic chains in the 1,2-di-*O*-alkyl- (▲, △) and 1,3-di-*O*-alkyl-glycerophosphocholine (■, □) series. * L represents the number of carbon atoms of the fluorinated tail (n) and hydrocarbon spacer (m) or of the hydrocarbon (m) alkyl chain.

compared to that of the F4 ones, prevents such a closer contact between the hydrophobic chains which is necessary to counterbalance the loss of hydrogen bonding.

Where the phase transition ΔH and ΔS parameters are concerned, it appears, as shown in Fig. 5a,b, that no significant trend can be evidenced when going from the ester to the ether series whether for the fluorinated or for the hydrocarbon derivatives.

3.4.2. Impact of the chain's position on glycerol (1,2- vs 1,3-isomer)

As shown in Fig. 6 for the Tc, no significant differences are found for the DF6C11OPC/1,3-DF6C11OPC and DF8C11OPC/1,3-DF8C11OPC pairs. This tendency parallels thus the trend established for the hydrocarbon series [17]. The 1,2-/1,3-isomerism also has no impact on the ΔH, ΔS parameters (see Tables 1 and 2).

3.4.3. Impact of the presence of fluorinated chains and of their number

The effect of the introduction of a fluorinated chain in a glycerophospholipidic structure on the thermodynamic parameters depends upon the number of chains (1 or 2), their length, the relative length of the fluorinated tail vs the whole length, i.e., the fluorination degree (defined as the ratio of the number of fluorinated carbons on the overall number of carbons constituting the hydrophobic chains).

Concerning Tc, as illustrated in Fig. 4a,b, our results show that, for comparable overall chain lengths L, the replacement of a hydrocarbon tail by its perfluorinated equivalent in both chains of the hydrocarbon glycerophosphocholines (whether they belong to the 1,2-, 1,3-ether or ester series [7]) induces an effect which is highly dependent upon the length of this tail. Thus, and in the 1,2-ether series, replacing a C8 by a F8 tail results in a large Tc increase: the Tc of DF8C5OPC (60°C for L = 13) is much higher than that of Tc of DC14OPC (27°C for L = 14) and even higher than that of DC18OPC (55°C, for L = 18) which has much longer chains. On the other hand, no significant effect on Tc is found when replacing a C6 for a F6 tail: the Tc of DF6C11OPC (50°C for L = 17) lies in between that of DC16OPC and DC18OPC. By contrast, a Tc decrease is evidenced when replacing a C4 for a F4 tail: thus and despite a longer chain length, DF4C11OPC (L = 15) displays a lower Tc (17°C) than DC14OPC. In the PE series and as illustrated in Fig. 4c, the tendencies evidenced in the PC series are also found for the F8 and F4 tails but a Tc decrease is observed for a F6 tail.

However, the replacement of a hydrocarbon tail by its perfluorinated equivalent in only one chain of the hydrocarbon glycerophosphocholines results systematically in a Tc decrease and this even for the longest F8 tail. This is illustrated in Fig. 7 which shows that the three fluorocarbon/hydrocarbon mixed-chain derivatives possess a Tc which is lower than that of their closest fully hydrocarbon analog. Conversely, the replacement of one of the two perfluoroalkylated chains in the fluorocarbon/fluorocarbon 1,3-DFnC11OPCs by a long C16 or C18 hydrocarbon chain diminishes significantly the Tc (Fig. 7); as an example, one can notice that the Tc of 1,3-[F8C11][C18]OPC lies far below (by almost 40°C) that of 1,3-DF8C11OPC. A similar result has also been evidenced for triple-chain fluorocarbon (respectively, hydrocarbon) ammonium amphiphiles where the replacement of one fluorocarbon (resp. hydrocarbon) chain by a hydrocarbon (resp. fluorocarbon) one resulted in a decrease of Tc [27].

Where the impact on Tc of the chain length increase is concerned, one can see, as illustrated in Fig. 4a–c and 7, that the Tc rises (1) on increasing the Fn

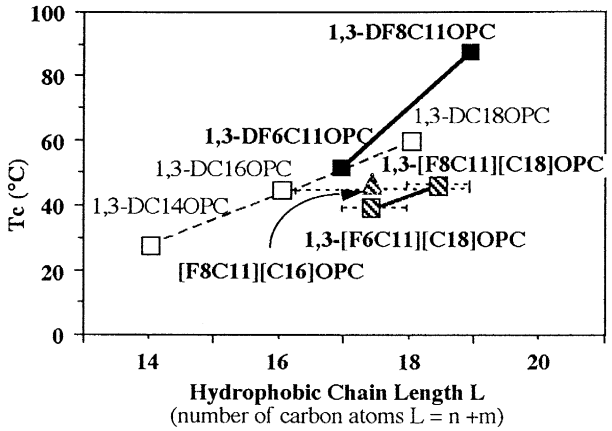

Fig. 7. Evolution of the phase transition temperature, Tc, with the length, L, of the hydrophobic chains in the fluorocarbon/fluorocarbon (filled symbols), hydrocarbon/hydrocarbon (open symbols) and mixed fluorocarbon/hydrocarbon (hatched symbols) di-*O*-alkyl-glycerophosphocholine series. * For the two former series, L represents the number of carbon atoms of the fluorinated tail (n) and hydrocarbon spacer (m) or of the hydrocarbon (m) alkyl chain. For the mixed series, L is the mean number of carbon atoms ($= n + m + m'/2$).

tail's length for a given Cm spacer: Tc of DF8C11OPC (or OPE) > Tc of DF6C110PC (or OPE) > Tc of DF4C11OPC (or OPE); (2) on increasing the Cm spacer's length for a given Fn tail (Tc of DF8C11OPC > Tc of DF8C5OPC). A similar correlation between Tc, which is closely connected to the melting of the hydrophobic chains, and the alkyl-chain's length is observed for the hydrocarbon glycerophosphocholines [18,19]. In the latter series, it was found that a monotonic chain lengthening of two methylenic carbon atoms is accompanied by a nearly monotonic Tc increase of about 20°C (Fig. 4c). By contrast, a chain lengthening of two CF_2s in the DFnC11OPC, DFnC11OPE (Fig. 4c) or 1,3-DFnC11OPC (Fig. 4b or Fig. 7) series results in a larger Tc increase ($\sim$ 30°C). An elongation by two CF_2s on only one chain also results in a Tc increase but the magnitude is less important: thus, the Tc's of 1,3-[F6C11][C18] and 1,3-[DF8C11][C18]OPC differ by only 8°C (Fig. 7).

A comparison between the Tc values of DF8C5OPC, DF4C11OPC and DF6C11OPC shows that the chain melting phase transition temperature is mainly modulated by the length of the Fn segment rather than by the overall chain length L (Fig. 4), hence by the fluorination degree. It was indeed expected that, when considering only L and by analogy with the hydrocarbon series, the phase transition of DF8C5OPC (L = 13) should be lower than that of DF4C11OPC (L = 15) and even of DF6C11OPC (L = 17). In fact, of the three compounds, it is DF8C5OPC which has the shortest chain length but the longest perfluoroalkyl tail, and, consequently, the highest fluorination degree, which displays the highest Tc. These results are in line with our previous study concerning their ester analogs [6,7].

Where the ΔH and ΔS parameters are concerned and as illustrated in Fig. 5a–f, it appears that the fluorinated (1,3-)DFnCmOPC, DFnCmOPE, [FnCm][Fn′Cm′]OPC and [FnCm][Cm′]OPC lamellar phases display much lower ΔH and ΔS values than their corresponding hydrocarbon ones. This behavior is similar to that evidenced for the fluorinated DFnCmPC phosphatidylcholines as compared to the hydrocarbon ones [7]. One should notice that the mixed fluorocarbon/hydrocarbon 1,3-[FnC11][C18]OPCs display intermediate ΔH and ΔS values to those measured for the fluorocarbon/fluorocarbon 1,3-DFnC11OPCs and fully hydrocarbon 1,3-DC18OPC. Furthermore, it is 1,3-[F6C11][C18]OPC which has the lowest fluorination degree among all the fluorinated compounds investigated here which displays the largest ΔH and ΔS values. All these results indicate that the transition is mainly due to the reorganization of the hydrocarbon Cm part of the FnCm chains and is further in line with studies performed on other fluorocarbon amphiphiles [28].

The ΔH and ΔS values in the hydrocarbon series, excepted for the 1,3-diether series, are seen to increase nearly linearly with increasing chain length (Fig. 5a–c and Fig. 5d–f), reflecting that the packing interactions are raising proportionally to the chain length increase. This is also the case in the DFnCm(O)PCs series (Fig. 5a,d), for which the ΔH and ΔS values are raising on increasing the Fn tail or the Cm spacer lengths. This tendency is not as evident in the 1,3- and PE series (Fig. 5b,e and 5c,f, respectively). It is therefore difficult to rationalize our results in terms of ΔH and ΔS increment per CF_2 and per CH_2 groups.

Owing to the geometric, electronic and hydrophobic characteristics which differentiate a hydrocarbon from a perfluoroalkyl chain, one expects that the

introduction in a membrane forming double-chain amphiphile of one or two fluorocarbon chains induces two antagonist effects on the thermodynamic Tc, ΔH and ΔS parameters of this membrane: (1) enhancement of packing disorder or fluidity, which results in a lowering in the thermodynamic parameter values, due mainly to weaker lateral inter- and intramolecular interactions and increased steric repulsions between the fluorocarbon chains or between a fluorocarbon and hydrocarbon chain, as compared with those existing between hydrocarbon chains [4], and (2) increase in order or rigidity, which is only expressed here by an augmentation of Tc, related to an increase in hydrophobic interactions [29]. In the case of the phospholipids having in both of their chains a short F4 (C_4F_9) perfluoroalkyl tail, the hydrophobic interactions are not likely to be sufficient to counterbalance the opposite effect. Thus, the replacement of part of the hydrocarbon chains by a F4 tail appears to induce membrane fluidification. A F6 (C_6F_{13}) tail is sufficient in some cases to equilibrate the antagonist contributions and does not modify membrane fluidity. By contrast a F8 (C_8F_{17}) segment results in the predominance of the hydrophobic interactions and enhances the membrane's rigidity. These results are found whatever the series (ester, 1,2- or 1,3-ether, PC or PE) to which the fluorinated phospholipids belong.

However, in the case of the mixed fluorocarbon/hydrocarbon phospholipids, the hydrophobic interactions induced by a F8 tail are not strong enough to compensate for weaker intermolecular fluorocarbon/fluorocarbon and intra- and intermolecular fluorocarbon/hydrocarbon chain–chain interactions [4] and increased steric repulsions [25,26]. The presence of one fluorocarbon together with a hydrocarbon chain thus results in a Tc decrease.

3.4.4. Impact of a double bond in the hydrocarbon spacer

It is well established that membranes formed from unsaturated phospholipids having a double bond in one and/or in both chains, (whether of *cis* or *trans* configuration) display much lower Tcs, as compared to membranes formed from their saturated analogs [2,18–20]. This is due to geometric perturbations imposed by the double bond on the overall conformation of a linear long aliphatic chain which are more important when the double bond is *cis* rather than *trans*.

In the case of the fluorocarbon unsaturated PCs ([F8E5][C14]OPC, [F8E11][C16]OPC and DF8E5OPC), these compounds consist in fact in a mixture of *cis* and, mainly, *trans* isomers (*cis*/*trans* $\leq 20/80$). The observed effects on the thermodynamic parameters will thus also depend upon the relative proportion of *cis*/*trans* isomers. The presence of a double bond in only one chain, as in [F8E11][C16]OPC, which is the sole compound of the unsaturated ones for which a phase transition has been detected, is found to be accompanied by a consequent decrease of Tc, from 44°C for the saturated [F8C11][C16]OPC to 5°C for [F8E11][C16]OPC. This trend is thus similar to what is usually found for the unsaturated/saturated phospholipids.

3.4.5. Symmetric vs. mixed fluorocarbon / fluorocarbon phospholipids

It is also interesting to compare the Tcs of the mixed fluorocarbon/fluorocarbon [F4C11][F8C11]OPC and [F8C5][F4C11]OPC phospholipids with those of 'symmetric' fluorocarbon/fluorocarbon DFnCmOPC ones.

The former mixed fluorocarbon/fluorocarbon [F4C11][F8C11]OPC possesses chains which differ by the length of their fluorinated tails and by their overall chain length (4 carbon atoms) [F4C11][F8C11]OPC results formally from the replacement of one of the F8 or F4 tails in the symmetric DF8C11OPC or DF4C11OPC, respectively. These replacements, which correspond to a chain shortening or lengthening by a F4 segment, respectively, are accompanied, as expected, by a Tc decrease (48°C) or increase (23°C), respectively. Although these results are in line with those already commented on above concerning the impact of a Fn tail length decrease/increase on Tc (see Section 3.4.3.), one can furthermore notice that two consecutive chain lengthenings by F4, hence when going from DF4C11OPC to [F4C11][F8C11]OPC then to DF8C11OPC, result in a significant difference in magnitude of Tc increase, the second one (48°C) being much larger than the former one (23°C). Such an increase in rigidity is mostly related to the larger hydrophobicity of the F8 compared to a F4 segment and, to a lesser extent, to

increased chain–chain interactions when both chains are of a similar length.

It is also interesting to note that the mixed [F4C11][F8C11]OPC displays a lower Tc (by 9°C) than the symmetric DF6C11OPC, although both compounds possess the same number (12) of fluorinated carbons and the same overall number of carbon atoms (34). A similar difference in Tc has also been reported in the hydrocarbon series, where it was found that the Tc of the mixed [C15][C19]PC (an analog of [F4C11][F8C11]OPC; see structure in Fig. 1) is lower (by 5°C) than that of the symmetric DC17PC (an analog of DF6C11OPC) [18]. These differences in Tc are most likely related to a difference in length (4 carbon atoms) between both chains in the mixed [F4C11][F8C11]OPC or [C15][C19]PC which results in a poorer chain–chain overlap and, consequently, in lower chain–chain interactions compared to, respectively, DF6C11OPC or DC17PC where both chains are of identical length. This is further supported by the non-ideal mixing behavior of DF4C11PC and DF6C11PC (whose chains differ by 2 fluorinated carbons) [30] or of DMPC and DSPC [31] (whose chains differ by 4 carbons) or by the thermodynamic preference for DMPC to become in closer contact of another DMPC in a mixed DMPC/DSPC bilayer [32].

The second mixed fluorocarbon/fluorocarbon [F8C5][F4C11]OPC possesses chains which differ by the length of both the fluorinated tails and hydrocarbon spacers. [F8C5][F4C11]OPC (Tc ~ 10°C) results formally from the replacement of a F8C5 chain in

Table 4
Vesicle size and size distribution for various formulations after preparation, heat-sterilization and storage at 25 ± 1°C

Liposome composition [a]	After preparation		After sterilization [b]		After storage at 25°C (±1°C)		
	Diameter (±S.D.) (nm)	Weight distribution (%)	Diameter (±S.D.) (nm)	Weight distribution (%)	Diameter (±S.D.) (nm)	Weight distribution (%)	Storage (days)
DF4C11OPC [d,e]	110 (70)	100	–	–	60 (15)	36	600
					210 (55)	64	
DF6C11OPC	110 (60)	100	180 (60)	100	3000 (500)	100	10
					deposit		30
[F8E11][C16]OPC	100 (15)	100	100 (15)	100	120 (25)	100	300
[F4C11][F8C11]OPC	140 (40)	100	125 (35)	100	110 (20)	60	100
					390 (150)	40	
					150 (45)	40	300
					700 (200)	60	
1,3-[F6C11][C18]OPC	90 (20)	80	100 (20)	88	80 (25)	75	100
	400 (140)	20	560 (80)	12	390 (130)	25	
					90 (20)	20	300
					3700 (1200)	80	
1,2-[F8C11][C18]OPC	140 (45)	100	100 (20)	93	100 (36)	80	300
			300 (55)	7	750 (250)	20	
1,3-DF6C11OPC	100 (60)	100	180 (80)	47	430 (150)	3	1
			1100 (350)	53	3500 (1300)	97	deposit
DF4C11PC [e]	130 (large)	100	130 (50)	100	40 (15)	14	300
					120 (35)	86	
DFFC [e]	60 (25)	43	140 (20)	14		6	
	260 (70)	57	1150 (250)	60	deposit		
EPC/CH	130 (30)	100	deposit				
EPC	110 (25)	100	105 (25)	100	100 (25)	100	300

[a] 10 mM of the phospholipid in a Hepes buffer.
[b] 121°C, 10^5 Pa, 15 min.
[c] S.D. is the standard deviation; 95% of the population is corresponding to ±1.96 S.D.
[d] not sterilized.
[e] From Ref. [8].

DF8C5OPC (Tc = 60°C) for a F4C11 one, which is accompanied by a Tc decrease (50°C). This Tc decrease was expected in view of the lower hydrophobicity of a F4(C11) chain compared to a F8(C5) one (see Section 3.4.3.). It is therefore surprising that, conversely, the replacement of a F4C11 chain in DF4C11OPC (Tc = 17°C) for a F8C5 one is accompanied by a Tc decrease (~ 7°C). This is most probably related to a difference in length between the two C5 and C11 hydrocarbon spacers in the mixed [F8C5][F4C11]OPC which, when packed in the bilayer, results in a subsequent overlap of the F8 tails with the C11 spacer neighbours and, consequently, in much lower F8C5/F4C11 chain–chain interactions than those existing between F4C11 chains. These lower F8C5/F4C11 chain–chain interactions are not compensated by the larger hydrophobic interactions developed by the F8(C5) chain, thus increasing membrane fluidity as compared to DF4C11OPC.

3.5. Long-term shelf stability of the fluorinated liposomes

The use of liposomes as a drug carrier system requires the development of heat-sterilizable and long-term shelf-stable formulations in terms of particle size and particle size distribution. Particle size is indeed a crucial parameter, among others, which governs the in vivo fate of the liposomes [1]. Vesicles made from pure monodispersed phospholipids have low stability. The development of more stable liposomes usually involves multicomponent systems and elaborate formulations. By contrast, we have previously shown that the fluorinated DFnCmPC phosphatidylcholines, as single components, form heat-sterilizable vesicles of exceptional shelf stability [8]. In this respect, it was of particular interest to examine the behavior of the liposomes formed from the new fluorinated di-*O*-alkylglycerophosphocholines, i.e., DF4C11OPC, DF6C11OPC, [F4C11][F8C11]OPC, [F8E11][C16]OPC, 1,3-[F6C11][C18]OPC, 1,3-[F8C11][C18]OPC and 1,3-DF6C11OPC, each of these compounds being representative of a series of phospholipids which have been synthesized.

Table 4 collects the mean diameters of the liposomal dispersions which have been measured by LSS, before and after heat sterilization (standard norms) and after storage at 25 ± 1°C for periods up to 600 days.

Most of the liposomes formed from the fluorinated ether-PCs can be thermally sterilized and stored at room temperature for several months without any significant modification of their mean size and size distribution. This is the case whether their membranes are in the fluid or gel state at the storage temperature, and formed from compounds having one or two fluorocarbon chains connected to glycerol in 1,2 or 1,3. These results confirm the remarkable stability of the fluorinated liposomes which contrasts strongly with that of most of the conventional liposomes (see Table 4). As evidenced by LSS, the fluorinated DF4C11OPC and [F8E11][C16]OPC liposomes, whose membranes are at 25°C in the fluid state, do indeed display no significant modifications in size and size distribution as those formed from their ester DF4C11PC analog. This reveals a rather exceptional stability of these liposomes when submitted to such a drastic sterilization procedure and/or to a storage period for up to 300 or 600 days. This is also the case of the conventional EPC liposomes which are, however, a polydispersed system.

For the fluorinated liposomes whose membranes are in the gel state at 25°C, the thermal sterilization process implies that they go through their phase transition. It appears that, for the fluorinated DF6C11OPC, [F4C11][F8C11]OPC, 1,3-[F6C11][C18]OPC and 1,3-[F8C11][C18]OPC liposomes, only minor changes in terms of particle size and size distribution are detected. Most of these formulations can also be stored for several months at room temperature, except DF6C11OPC which forms larger aggregates and precipitates after only a one-month storage period, and 1,3-DF6C11OPC which displays even a much lower stability. The poorer stability of these two latter fluorinated formulations may be related to the formation of a ribbon-like phase from the lamellar gel phase, as detected by FFEM (vide supra). The much greater stability of the former fluorinated liposomes contrasts strongly with that of the conventional 'gel' DPPC or EPC/CH 1/1 liposomes for which a precipitate is formed after a shorter period of storage or immediately after sterilization, respectively (see Table 4).

The stability in terms of size and size distribution of the fluorinated liposomes seems to be a character-

istic of such systems as it has also been observed for a large series of fluorinated amphiphiles [33]. This could arise from the increased hydrophobic character induced by the presence of the perfluoroalkyl tails [4] and consequently of the intramembranous fluorocarbon film [6], although replacing part of a hydrocarbon tail by a perfluoroalkyl one reduces the inter- and intramolecular chain–chain interactions [4] and increases steric repulsions [25,26]. It appears that the associative forces which nevertheless exist between the fluorocarbon hydrophobic chains and, more importantly, the hydrophobic interactions are sufficient to maintain a stable closed bilayer structure in water. In this respect, it should be mentioned that the presence of only one fluorocarbon chain (as in 1,3-[F6C11][C18]OPC and 1,3-[F8C11][C18]OPC) still improves the vesicle's shelf stability.

Acknowledgements

This work was supported by the CNRS of France. We thank Dr. T. Gulik-Krzywicki for helpful discussions, Dr. B. Monasse and J.-P. Rolland for assistance with the DSC measurements.

References

[1] Gregoriadis, G. (1993) in Liposome Technology, Vols. I–III, 2nd edn., CRC Press, Boca Raton.
[2] Lasic, D.D. (1993) in Liposomes: From Physics to Applications, Elsevier, Amsterdam.
[3] Lasic, D.D. (1994) Angew. Chem., Int. Ed. Engl. 33, 1685–1698.
[4] Mukerjee, P. and Handa, I. (1981) J. Phys. Chem. 85, 2298–2303.
[5] Santaella, C., Vierling, P. and Riess, J.G. (1991) New. J. Chem. 15, 685–692.
[6] Vierling, P., Santaella, C. and Riess, J.G. (1995) in Liposomes: New Systems and New Trends in their Applications (Puisieux, F., Couvreur, P., Delattre, J. and Devissaguet, J.P., eds.), pp. 293–318, Edition de Santé, Paris.
[7] Santaella, C., Vierling, P., Riess, J.G., Gulik-Krzywicki, T., Gulik, A. and Monasse, B. (1994) Biochim. Biophys. Acta 1190, 25–39.
[8] Santaella, C., Vierling, P. and Riess, J.G. (1991) Angew. Chem., Int. Ed. Engl. 30, 567–568.
[9] Santaella, C. and Vierling. P. (1995) Chem. Phys. Lipids. 77, 173–177.
[10] (a) Frézard, F., Santaella, C., Vierling, P. and Riess, J.G. (1994) Biochim. Biophys. Acta 1192, 61–70; (b) Frézard, F., Santaella, C., Montisci, M.-J., Vierling, P. and Riess, J.G. (1994) Biochim. Biophys. Acta 1194, 61–68.
[11] Santaella, C., Frézard, F., Vierling, P. and Riess, J.G. (1993) FEBS Lett. 336, 481–483.
[12] Ravily, V., Gaentzler, S., Santaella, C. and Vierling, P. (1996) Helv. Chim. Acta 79, 405–425.
[13] Gulik, A., Santaella, C., Ravily, V. and Vierling, P. unpublished results.
[14] Kim, J.Y., Mattai, J. and Shipley, G.G. (1987) Biochemistry 26, 6592–6598.
[15] Serrallach, E.N., Dijkman, R., De Haas, G.H. and Shipley, G.G. (1983) J. Mol. Biol. 170, 155–174.
[16] McIntosh, T.J., Simon, S.A., Vierling, P., Santaella, C. and Ravily, V. (1996) Biophys. J., in press.
[17] Kunitake, T., Okahata, Y. and Tawaki, S.I. (1985) J. Coll. Int. Sci. 103, 190–201.
[18] Cevc, G. (1993) in Phospholipids Handbook, M. Dekker, New York.
[19] Dufourcq, J. (1985) in Les Liposomes, Applications Thérapeutiques (Puisieux, F. and Delattre, J., eds.), pp. 1–39, Technique et Documentation, Lavoisier, Paris.
[20] Cevc, G. (1991) Biochemistry 30, 7186–7193.
[21] Seddom, J.M., Cevc, G. and Marsh, D. (1983) Biochemistry 22, 1280–1290.
[22] Tardieu, A., Luzzati V. and Reman, F.C. (1973) J. Mol. Biol. 75, 711–733.
[23] Koyonova, R. and Caffrey, M. (1994) Chem. Phys. Lipids 69, 1–34.
[24] Vaughan, D.J. and Keough, K.M. (1974) FEBS Lett. 47, 158–161.
[25] Tiddy, G.J.T. (1985) in Modern Trends of Colloid Science in Chemistry and Biology (Eicke, H.F., ed.), pp. 148–183, Birkhäuser, Basel.
[26] Rosen, M.J., Cohen, A.W., Dahanayake, M. and Xi-Tuan Hua, J. (1982) J. Phys. Chem. 86, 541–545.
[27] Kunitake, T. and Higashi, N. (1985) J. Am. Chem. Soc. 107, 692–696.
[28] Kunitake, T., Ando, R. and Ishikawa, Y. (1986) Mem. Fac. Kyushu Univ. 46, 231–243.
[29] Hargreaves, W.R. and Deamer, D.W. (1978) Biochemistry 18, 3759–3768.
[30] Rolland, J.-P., Santaella, C., Vierling, P. and Monasse, B., Chem. Phys. Lipids, in press.
[31] Mabrey, S. and Sturtevant, J.M. (1976) Proc. Natl. Acad. Sci. USA 73, 3862–3866.
[32] Krisovitch, S.M. and Regen, S.L. (1991) J. Am. Chem. Soc. 113, 8176–8177.
[33] Riess, J.G., Frézard, F., Greiner, J., Krafft, M.-P., Santaella, C., Vierling, P. and Zarif, L. (1996) in Handbook of Non-Medical Applications of Liposomes, (Barenholtz, Y. and Lasic, D.D., eds.) Vol. III, pp. 97–141, CRC Press, Boca Raton (review).